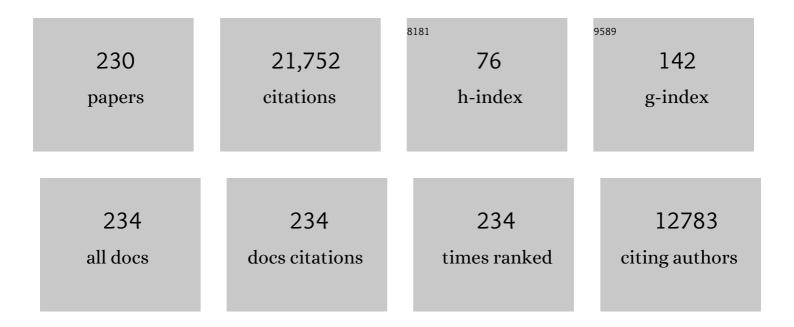
List of Publications by Year in descending order

Source: https://exaly.com/author-pdf/7121524/publications.pdf Version: 2024-02-01



#	Article	IF	CITATIONS
1	The Interfield Strength Agreement of Left Ventricular Strain Measurements at 1. <scp>5ÂT</scp> and <scp>3ÂT</scp> Using Cardiac <scp>MRI</scp> Feature Tracking. Journal of Magnetic Resonance Imaging, 2023, 57, 1250-1261.	3.4	6
2	Distinct cardiovascular phenotypes are associated with prognosis in systemic sclerosis: a cardiovascular magnetic resonance study. European Heart Journal Cardiovascular Imaging, 2023, 24, 463-471.	1.2	7
3	Hypertrophic cardiomyopathy: insights from extracellular volume mapping. European Journal of Preventive Cardiology, 2022, 28, e39-e41.	1.8	6
4	Non-invasive characterization of pleural and pericardial effusions using T1 mapping by magnetic resonance imaging. European Heart Journal Cardiovascular Imaging, 2022, 23, 1117-1126.	1.2	8
5	Evaluation of Hepatic Iron Overload Using a Contemporary 0. <scp>55 T MRI</scp> System. Journal of Magnetic Resonance Imaging, 2022, 55, 1855-1863.	3.4	4
6	Phenotyping hypertrophic cardiomyopathy using cardiac diffusion magnetic resonance imaging: the relationship between microvascular dysfunction and microstructural changes. European Heart Journal Cardiovascular Imaging, 2022, 23, 352-362.	1.2	12
7	Diffusely Increased Myocardial Extracellular Volume With or Without Focal Late Gadolinium Enhancement. Journal of Thoracic Imaging, 2022, 37, 17-25.	1.5	4
8	Effective Study: Development and Application of a Questionâ€Driven, Timeâ€Effective Cardiac Magnetic Resonance Scanning Protocol. Journal of the American Heart Association, 2022, 11, e022605.	3.7	1
9	Automated Inâ€Line Artificial Intelligence Measured Global Longitudinal Shortening and Mitral Annular Plane Systolic Excursion: Reproducibility and Prognostic Significance. Journal of the American Heart Association, 2022, 11, e023849.	3.7	11
10	Improved accuracy and precision with threeâ€parameter simultaneous myocardial T ₁ and T ₂ mapping using multiparametric SASHA. Magnetic Resonance in Medicine, 2022, 87, 2775-2791.	3.0	13
11	Quantitative Myocardial Perfusion Predicts Outcomes in Patients With Prior SurgicalÂRevascularization. Journal of the American College of Cardiology, 2022, 79, 1141-1151.	2.8	10
12	Coronary microvascular function and visceral adiposity in patients with normal body weight and type 2 diabetes. Obesity, 2022, 30, 1079-1090.	3.0	7
13	Study protocol: MyoFit46—the cardiac sub-study of the MRC National Survey of Health and Development. BMC Cardiovascular Disorders, 2022, 22, 140.	1.7	4
14	Association of ambulatory blood pressure with coronary microvascular and cardiac dysfunction in asymptomatic type 2 diabetes. Cardiovascular Diabetology, 2022, 21, .	6.8	5
15	Reduction in CMR Derived Extracellular Volume With Patisiran Indicates Cardiac Amyloid Regression. JACC: Cardiovascular Imaging, 2021, 14, 189-199.	5.3	113
16	Quantitative cardiovascular magnetic resonance myocardial perfusion mapping to assess hyperaemic response to adenosine stress. European Heart Journal Cardiovascular Imaging, 2021, 22, 273-281.	1.2	15
17	Measurement of T1 Mapping in Patients With Cardiac Devices: Off-Resonance Error Extends Beyond Visual Artifact but Can Be Quantified and Corrected. Frontiers in Cardiovascular Medicine, 2021, 8, 631366.	2.4	6
18	Patterns of myocardial injury in recovered troponin-positive COVID-19 patients assessed by cardiovascular magnetic resonance. European Heart Journal, 2021, 42, 1866-1878.	2.2	274

#	Article	IF	CITATIONS
19	A comparison of standard and high dose adenosine protocols in routine vasodilator stress cardiovascular magnetic resonance: dosage affects hyperaemic myocardial blood flow in patients with severe left ventricular systolic impairment. Journal of Cardiovascular Magnetic Resonance, 2021, 23, 37.	3.3	11
20	Freeâ€breathing simultaneous <i>T</i> ₁ , <i>T</i> ₂ , and <i>T</i> ₂ ^{â^—} quantification in the myocardium. Magnetic Resonance in Medicine, 2021, 86, 1226-1240.	3.0	11
21	Cardiac Magnetic Resonance–Derived Extracellular Volume Mapping for the Quantification of Hepatic and Splenic Amyloid. Circulation: Cardiovascular Imaging, 2021, 14, CIRCIMAGING121012506.	2.6	19
22	Prognostic Value of Pulmonary Transit Time and Pulmonary Blood Volume Estimation Using Myocardial PerfusionÂCMR. JACC: Cardiovascular Imaging, 2021, 14, 2107-2119.	5.3	18
23	Prospective Case-Control Study of Cardiovascular Abnormalities 6ÂMonthsÂFollowing Mild COVID-19 inÂHealthcare Workers. JACC: Cardiovascular Imaging, 2021, 14, 2155-2166.	5.3	111
24	Recurrent acute pericarditis diagnosed by extra-cellular volume maps. European Heart Journal, 2021, , .	2.2	0
25	Use of quantitative cardiovascular magnetic resonance myocardial perfusion mapping for characterization of ischemia in patients with left internal mammary coronary artery bypass grafts. Journal of Cardiovascular Magnetic Resonance, 2021, 23, 82.	3.3	6
26	Myocardial Perfusion Defects in Hypertrophic Cardiomyopathy Mutation Carriers. Journal of the American Heart Association, 2021, 10, e020227.	3.7	15
27	Landmark Detection in Cardiac MRI by Using a Convolutional Neural Network. Radiology: Artificial Intelligence, 2021, 3, e200197.	5.8	24
28	Clinical associations with stage B heart failure in adults with type 2 diabetes. Therapeutic Advances in Endocrinology and Metabolism, 2021, 12, 204201882110301.	3.2	2
29	Empagliflozin Treatment Is Associated With Improvements in Cardiac Energetics and Function and Reductions in Myocardial Cellular Volume in Patients With Type 2 Diabetes. Diabetes, 2021, 70, 2810-2822.	0.6	36
30	Bright-blood and dark-blood phase sensitive inversion recovery late gadolinium enhancement and T1 and T2 maps in a single free-breathing scan: an all-in-one approach. Journal of Cardiovascular Magnetic Resonance, 2021, 23, 126.	3.3	7
31	Progressive myocardial injury in myotonic dystrophy type II and facioscapulohumeral muscular dystrophy 1: a cardiovascular magnetic resonance follow-up study. Journal of Cardiovascular Magnetic Resonance, 2021, 23, 130.	3.3	3
32	Myocardial Perfusion Imaging After Severe COVID-19 Infection Demonstrates Regional Ischemia Rather Than Global Blood Flow Reduction. Frontiers in Cardiovascular Medicine, 2021, 8, 764599.	2.4	9
33	Extracellular Volume Associates WithÂOutcomes More Strongly Than Native or Post-Contrast Myocardial T1. JACC: Cardiovascular Imaging, 2020, 13, 44-54.	5.3	68
34	Automatic inâ€line quantitative myocardial perfusion mapping: Processing algorithm and implementation. Magnetic Resonance in Medicine, 2020, 83, 712-730.	3.0	27
35	Noncontrast Magnetic Resonance for theÂDiagnosis of Cardiac Amyloidosis. JACC: Cardiovascular Imaging, 2020, 13, 69-80.	5.3	125
36	COVID-19. Circulation, 2020, 142, 1120-1122.	1.6	126

#	Article	IF	CITATIONS
37	Cardiovascular Determinants of Aerobic Exercise Capacity in Adults With Type 2 Diabetes. Diabetes Care, 2020, 43, 2248-2256.	8.6	25
38	The Chief Scientist Office Cardiovascular and Pulmonary Imaging in SARS Coronavirus disease-19 (CISCO-19) study. Cardiovascular Research, 2020, 116, 2185-2196.	3.8	31
39	Automated Inline Analysis of Myocardial Perfusion MRI with Deep Learning. Radiology: Artificial Intelligence, 2020, 2, e200009.	5.8	32
40	A comparison of cine CMR imaging at 0.55 T and 1.5 T. Journal of Cardiovascular Magnetic Resonance, 2020, 22, 37.	3.3	25
41	Automated detection of left ventricle in arterial input function images for inline perfusion mapping using deep learning: A study of 15,000 patients. Magnetic Resonance in Medicine, 2020, 84, 2788-2800.	3.0	19
42	T1 mapping performance and measurement repeatability: results from the multi-national T1 mapping standardization phantom program (T1MES). Journal of Cardiovascular Magnetic Resonance, 2020, 22, 31.	3.3	23
43	Extracellular Volume and Global Longitudinal Strain Both Associate WithÂOutcomes But Correlate Minimally. JACC: Cardiovascular Imaging, 2020, 13, 2343-2354.	5.3	42
44	Inline perfusion mapping provides insights into the disease mechanism in hypertrophic cardiomyopathy. Heart, 2020, 106, 824-829.	2.9	26
45	Females have higher myocardial perfusion, blood volume and extracellular volume compared to males – an adenosine stress cardiovascular magnetic resonance study. Scientific Reports, 2020, 10, 10380.	3.3	39
46	The Prognostic Significance of Quantitative Myocardial Perfusion: An Artificial Intelligence Based Approach Using Perfusion Mapping. Circulation, 2020, 141, 1282-1291.	1.6	100
47	Assessment of Multivessel Coronary Artery Disease Using Cardiovascular Magnetic Resonance Pixelwise Quantitative Perfusion Mapping. JACC: Cardiovascular Imaging, 2020, 13, 2546-2557.	5.3	30
48	Improved Workflow for Quantification of Right Ventricular Volumes Using Free-Breathing Motion Corrected Cine Imaging. Pediatric Cardiology, 2019, 40, 79-88.	1.3	8
49	Quantitative Myocardial Perfusion in Fabry Disease. Circulation: Cardiovascular Imaging, 2019, 12, e008872.	2.6	32
50	Opportunities in Interventional and Diagnostic Imaging by Using High-Performance Low-Field-Strength MRI. Radiology, 2019, 293, 384-393.	7.3	224
51	The Effect of Blood Composition on T1ÂMapping. JACC: Cardiovascular Imaging, 2019, 12, 1888-1890.	5.3	9
52	Quantitative myocardial perfusion in coronary artery disease: A perfusion mapping study. Journal of Magnetic Resonance Imaging, 2019, 50, 756-762.	3.4	35
53	Interrogation of the infarcted and salvaged myocardium using multi-parametric mapping cardiovascular magnetic resonance in reperfused ST-segment elevation myocardial infarction patients. Scientific Reports, 2019, 9, 9056.	3.3	1
54	Detection of myocarditis using T 1 and ECV mapping is not improved by early compared to late postâ€contrast imaging. Clinical Physiology and Functional Imaging, 2019, 39, 384-392.	1.2	4

#	Article	IF	CITATIONS
55	Motion-corrected free-breathing LGE delivers high quality imaging and reduces scan time by half: an independent validation study. International Journal of Cardiovascular Imaging, 2019, 35, 1893-1901.	1.5	22
56	Subclinical myocardial injury in patients with Facioscapulohumeral muscular dystrophy 1 and preserved ejection fraction – assessment by cardiovascular magnetic resonance. Journal of Cardiovascular Magnetic Resonance, 2019, 21, 25.	3.3	17
57	Acute changes in cardiac structural and tissue characterisation parameters following haemodialysis measured using cardiovascular magnetic resonance. Scientific Reports, 2019, 9, 1388.	3.3	27
58	Automated Pixel-Wise Quantitative Myocardial Perfusion Mapping by CMRÂtoÂDetect Obstructive Coronary Artery Disease and Coronary Microvascular Dysfunction. JACC: Cardiovascular Imaging, 2019, 12, 1958-1969.	5.3	140
59	The relative contributions of myocardial perfusion, blood volume and extracellular volume to native T1 and native T2 at rest and during adenosine stress in normal physiology. Journal of Cardiovascular Magnetic Resonance, 2019, 21, 73.	3.3	24
60	Clinical impact of cardiovascular magnetic resonance with optimized myocardial scar detection in patients with cardiac implantable devices. International Journal of Cardiology, 2019, 279, 72-78.	1.7	29
61	A framework for constraining image SNR loss due to MR raw data compression. Magnetic Resonance Materials in Physics, Biology, and Medicine, 2019, 32, 213-225.	2.0	1
62	Validation of cardiac magnetic-resonance-derived left ventricular strain measurements from free-breathing motion-corrected cine imaging. Pediatric Radiology, 2019, 49, 68-75.	2.0	2
63	Native T1 and Extracellular Volume inÂTransthyretin Amyloidosis. JACC: Cardiovascular Imaging, 2019, 12, 810-819.	5.3	172
64	Simultaneous 13N-Ammonia and gadolinium first-pass myocardial perfusion with quantitative hybrid PET-MR imaging: a phantom and clinical feasibility study. European Journal of Hybrid Imaging, 2019, 3, 15.	1.5	10
65	Techniques for T1, T2, and Extracellular Volume Mapping. , 2019, , 15-26.e2.		Ο
66	Myocardial native T1 and extracellular volume with healthy ageing and gender. European Heart Journal Cardiovascular Imaging, 2018, 19, 615-621.	1.2	78
67	Reverse Myocardial Remodeling FollowingÂValve Replacement in PatientsÂWith Aortic Stenosis. Journal of the American College of Cardiology, 2018, 71, 860-871.	2.8	266
68	Dark-Blood Late-Enhancement ImagingÂImproves Detection of Myocardial Infarction. JACC: Cardiovascular Imaging, 2018, 11, 1770-1772.	5.3	10
69	Blood volume measurement using cardiovascular magnetic resonance and ferumoxytol: preclinical validation. Journal of Cardiovascular Magnetic Resonance, 2018, 20, 62.	3.3	9
70	Fully automated, inline quantification of myocardial blood flow with cardiovascular magnetic resonance: repeatability of measurements in healthy subjects. Journal of Cardiovascular Magnetic Resonance, 2018, 20, 48.	3.3	54
71	Detection of Recent Myocardial Infarction Using Native T1 Mapping in a Swine Model: A Validation Study. Scientific Reports, 2018, 8, 7391.	3.3	18
72	Myocardial Edema and Prognosis inÂAmyloidosis. Journal of the American College of Cardiology, 2018, 71, 2919-2931.	2.8	145

#	Article	lF	CITATIONS
73	Characterization of T ₁ bias in skeletal muscle from fat in MOLLI and SASHA pulse sequences: Quantitative fatâ€fraction imaging with T ₁ mapping. Magnetic Resonance in Medicine, 2017, 77, 237-249.	3.0	25
74	Detection and Monitoring of Acute Myocarditis Applying Quantitative Cardiovascular Magnetic Resonance. Circulation: Cardiovascular Imaging, 2017, 10, .	2.6	100
75	Acute Cardiac MRI Assessment of Radiofrequency Ablation Lesions for Pediatric Ventricular Arrhythmia: Feasibility and Clinical Correlation. Journal of Cardiovascular Electrophysiology, 2017, 28, 517-522.	1.7	14
76	Assessment of Myocardial Microstructural Dynamics by InÂVivo Diffusion Tensor Cardiac Magnetic Resonance. Journal of the American College of Cardiology, 2017, 69, 661-676.	2.8	171
77	Myocardial extracellular volume fraction quantified by cardiovascular magnetic resonance is increased in hypertension and associated with left ventricular remodeling. European Radiology, 2017, 27, 4620-4630.	4.5	26
78	Late Anthracycline-Related Cardiotoxicity in Low-Risk Breast Cancer Patients. Journal of the American College of Cardiology, 2017, 69, 2573-2575.	2.8	12
79	Simultaneous multislice imaging for native myocardial T ₁ mapping: Improved spatial coverage in a single breath-hold. Magnetic Resonance in Medicine, 2017, 78, 462-471.	3.0	32
80	Assessing for Cardiotoxicity from Metal-on-Metal Hip Implants with Advanced Multimodality Imaging Techniques. Journal of Bone and Joint Surgery - Series A, 2017, 99, 1827-1835.	3.0	21
81	Magnetic Resonance in TransthyretinÂCardiac Amyloidosis. Journal of the American College of Cardiology, 2017, 70, 466-477.	2.8	290
82	Temporal Relation Between Myocardial Fibrosis and Heart Failure With Preserved Ejection Fraction. JAMA Cardiology, 2017, 2, 995.	6.1	164
83	Clinical recommendations for cardiovascular magnetic resonance mapping of T1, T2, T2* and extracellular volume: A consensus statement by the Society for Cardiovascular Magnetic Resonance (SCMR) endorsed by the European Association for Cardiovascular Imaging (EACVI). Journal of Cardiovascular Magnetic Resonance. 2017. 19. 75.	3.3	1,074
84	Diffuse myocardial fibrosis among healthy pediatric heart transplant recipients: Correlation of histology, cardiovascular magnetic resonance, and clinical phenotype. Pediatric Transplantation, 2017, 21, e12986.	1.0	14
85	High Spatial Resolution Cardiovascular Magnetic Resonance at 7.0 Tesla in Patients with Hypertrophic Cardiomyopathy – First Experiences: Lesson Learned from 7.0 Tesla. PLoS ONE, 2016, 11, e0148066.	2.5	28
86	Residual Myocardial Iron Following Intramyocardial Hemorrhage During the Convalescent Phase of Reperfused ST-Segment–Elevation Myocardial Infarction and Adverse Left Ventricular Remodeling. Circulation: Cardiovascular Imaging, 2016, 9, .	2.6	120
87	Quantification of Left Ventricular Function With Premature Ventricular Complexes Reveals Variable Hemodynamics. Circulation: Arrhythmia and Electrophysiology, 2016, 9, e003520.	4.8	20
88	Ultrafast Magnetic Resonance Imaging for Iron Quantification in Thalassemia Participants in the Developing World. Circulation, 2016, 134, 432-434.	1.6	23
89	Automated Extracellular Volume Fraction Mapping Provides Insights Into the Pathophysiology of Left Ventricular Remodeling Post–Reperfused STâ€Elevation Myocardial Infarction. Journal of the American Heart Association, 2016, 5, .	3.7	46
90	Cardiac Involvement in Myotonic Dystrophy Type 2 Patients With Preserved Ejection Fraction. Circulation: Cardiovascular Imaging, 2016, 9, .	2.6	41

#	Article	IF	CITATIONS
91	A medical device-grade T1 and ECV phantom for global T1 mapping quality assurance—the T1 Mapping and ECV Standardization in cardiovascular magnetic resonance (T1MES) program. Journal of Cardiovascular Magnetic Resonance, 2016, 18, 58.	3.3	134
92	Dark blood Late Gadolinium Enhancement improves conspicuity of ablation lesions. Journal of Cardiovascular Magnetic Resonance, 2016, 18, P211.	3.3	8
93	Improved workflow for quantification of left ventricular volumes and mass using free-breathing motion corrected cine imaging. Journal of Cardiovascular Magnetic Resonance, 2016, 18, 10.	3.3	24
94	Free-breathing motion-corrected late-gadolinium-enhancement imaging improves image quality in children. Pediatric Radiology, 2016, 46, 983-990.	2.0	20
95	Automatic Measurement of the MyocardialÂInterstitium. JACC: Cardiovascular Imaging, 2016, 9, 54-63.	5.3	127
96	Blood correction reduces variability and gender differences in native myocardial T1 values at 1.5ÂT cardiovascular magnetic resonance – a derivation/validation approach. Journal of Cardiovascular Magnetic Resonance, 2016, 19, 41.	3.3	21
97	Myocardial perfusion cardiovascular magnetic resonance: optimized dual sequence and reconstruction for quantification. Journal of Cardiovascular Magnetic Resonance, 2016, 19, 43.	3.3	185
98	Native T1 values identify myocardial changes and stratify disease severity in patients with Duchenne muscular dystrophy. Journal of Cardiovascular Magnetic Resonance, 2016, 18, 72.	3.3	51
99	Dark blood late enhancement imaging. Journal of Cardiovascular Magnetic Resonance, 2016, 18, 77.	3.3	64
100	CMR fluoroscopy right heart catheterization for cardiac output and pulmonary vascular resistance: results in 102 patients. Journal of Cardiovascular Magnetic Resonance, 2016, 19, 54.	3.3	41
101	Quantification of both the area-at-risk and acute myocardial infarct size in ST-segment elevation myocardial infarction using T1-mapping. Journal of Cardiovascular Magnetic Resonance, 2016, 19, 57.	3.3	41
102	Fully quantitative cardiovascular magnetic resonance myocardial perfusion ready for clinical use: a comparison between cardiovascular magnetic resonance imaging and positron emission tomography. Journal of Cardiovascular Magnetic Resonance, 2016, 19, 78.	3.3	110
103	Prospective comparison of novel dark blood late gadolinium enhancement with conventional bright blood imaging for the detection of scar. Journal of Cardiovascular Magnetic Resonance, 2016, 19, 91.	3.3	36
104	Saturation pulse design for quantitative myocardial T1 mapping. Journal of Cardiovascular Magnetic Resonance, 2015, 17, 84.	3.3	31
105	Characterization of myocardial T1-mapping bias caused by intramyocardial fat in inversion recovery and saturation recovery techniques. Journal of Cardiovascular Magnetic Resonance, 2015, 17, 33.	3.3	80
106	Increased myocardial extracellular volume in active idiopathic systemic capillary leak syndrome. Journal of Cardiovascular Magnetic Resonance, 2015, 17, 76.	3.3	17
107	Contrast-free detection of myocardial fibrosis in hypertrophic cardiomyopathy patients with diffusion-weighted cardiovascular magnetic resonance. Journal of Cardiovascular Magnetic Resonance, 2015, 17, 107.	3.3	48
108	Image reconstruction: An overview for clinicians. Journal of Magnetic Resonance Imaging, 2015, 41, 573-585.	3.4	43

#	Article	IF	CITATIONS
109	Noise propagation in region of interest measurements. Magnetic Resonance in Medicine, 2015, 73, 1300-1308.	3.0	8
110	Noncontrast myocardial <i>T</i> ₁ mapping using cardiovascular magnetic resonance for iron overload. Journal of Magnetic Resonance Imaging, 2015, 41, 1505-1511.	3.4	139
111	Variability of T1 in purpose recruited normal volunteers and patients as a function of shim (B0), flip angle (B1) and myocardial sector at 3T. Journal of Cardiovascular Magnetic Resonance, 2015, 17, P5.	3.3	3
112	Myocardial Fibrosis Quantified by Extracellular Volume Is Associated With Subsequent Hospitalization for Heart Failure, Death, or Both Across the Spectrum of Ejection Fraction and Heart Failure Stage. Journal of the American Heart Association, 2015, 4, .	3.7	174
113	FLASH proton density imaging for improved surface coil intensity correction in quantitative and semi-quantitative SSFP perfusion cardiovascular magnetic resonance. Journal of Cardiovascular Magnetic Resonance, 2015, 17, 16.	3.3	9
114	Mechanisms for overestimating acute myocardial infarct size with gadolinium-enhanced cardiovascular magnetic resonance imaging in humans: a quantitative and kinetic study. European Heart Journal Cardiovascular Imaging, 2015, 17, jev123.	1.2	30
115	Cardiac involvement of myotonic dystrophy type II in patients with preserved ejection fraction - Detection by CMR. Journal of Cardiovascular Magnetic Resonance, 2015, 17, P315.	3.3	0
116	Optimized saturation pulse rrains for SASHA T1 mapping at 3T. Journal of Cardiovascular Magnetic Resonance, 2015, 17, W20.	3.3	3
117	Automated inline extracellular volume (ECV) mapping. Journal of Cardiovascular Magnetic Resonance, 2015, 17, W6.	3.3	5
118	Free-breathing T2* mapping using respiratory motion corrected averaging. Journal of Cardiovascular Magnetic Resonance, 2015, 17, 3.	3.3	29
119	Myocardial T2* mapping: influence of noise on accuracy and precision. Journal of Cardiovascular Magnetic Resonance, 2015, 17, 7.	3.3	35
120	Temporal and spatial characteristics of the area at risk investigated using computed tomography and T ₁ -weighted magnetic resonance imaging. European Heart Journal Cardiovascular Imaging, 2015, 16, 1232-1240.	1.2	11
121	Prognostic Value of Late Gadolinium Enhancement Cardiovascular Magnetic Resonance in Cardiac Amyloidosis. Circulation, 2015, 132, 1570-1579.	1.6	442
122	Distributed MRI reconstruction using gadgetron-based cloud computing. Magnetic Resonance in Medicine, 2015, 73, 1015-1025.	3.0	50
123	Hemodynamic Consequences of Hypertrophic Cardiomyopathy with Midventricular Obstruction: Apical Aneurysm and Thrombus Formation. Journal of General Practice (Los Angeles, Calif), 2014, 02, .	0.1	5
124	Myocardial extracellular volume fraction quantified by cardiovascular magnetic resonance is increased in diabetes and associated with mortality and incident heart failure admission. European Heart Journal, 2014, 35, 657-664.	2.2	297
125	Accelerating Cardiovascular Magnetic Resonance Imaging: Signal Processing Meets Nuclear Spins [Life Sciences]. IEEE Signal Processing Magazine, 2014, 31, 138-143.	5.6	2
126	Accuracy, Precision, and Reproducibility of Four T1 Mapping Sequences: A Head-to-Head Comparison of MOLLI, ShMOLLI, SASHA, and SAPPHIRE. Radiology, 2014, 272, 683-689.	7.3	255

#	Article	IF	CITATIONS
127	Number of Pâ€Wave Fragmentations on Pâ€SAECG Correlates with Infiltrated Atrial Fat. Annals of Noninvasive Electrocardiology, 2014, 19, 114-121.	1.1	9
128	Method for calculating confidence intervals for phase contrast flow measurements. Journal of Cardiovascular Magnetic Resonance, 2014, 16, 46.	3.3	4
129	Free breathing myocardial perfusion data sets for performance analysis of motion compensation algorithms. GigaScience, 2014, 3, 23.	6.4	5
130	Reproducibility of native myocardial T1 mapping in the assessment of Fabry disease and its role in early detection of cardiac involvement by cardiovascular magnetic resonance. Journal of Cardiovascular Magnetic Resonance, 2014, 16, 99.	3.3	154
131	T1-mapping in the heart: accuracy and precision. Journal of Cardiovascular Magnetic Resonance, 2014, 16, 2.	3.3	551
132	Distinction of salvaged and infarcted myocardium within the ischaemic area-at-risk with T2 mapping. European Heart Journal Cardiovascular Imaging, 2014, 15, 1048-1053.	1.2	35
133	Cardiac involvement of the systemic disorder myotonic dystrophy type II - detection by CMR. Journal of Cardiovascular Magnetic Resonance, 2014, 16, P390.	3.3	О
134	Synthetic phase sensitive inversion recovery late gadolinium enhancement from post-contrast T1-mapping shows excellent agreement with conventional PSIR-LGE for diagnosing myocardial scar. Journal of Cardiovascular Magnetic Resonance, 2014, 16, P213.	3.3	3
135	Modular 32-channel transceiver coil array for cardiac MRI at 7.0T. Magnetic Resonance in Medicine, 2014, 72, 276-290.	3.0	90
136	Optimized saturation recovery protocols for T1-mapping in the heart: influence of sampling strategies on precision. Journal of Cardiovascular Magnetic Resonance, 2014, 16, 55.	3.3	42
137	Infiltrated atrial fat characterizes underlying atrial fibrillation substrate in patients at risk as defined by the ARIC atrial fibrillation risk score. International Journal of Cardiology, 2014, 172, 196-201.	1.7	26
138	Diagnostic Accuracy of Stress Perfusion CMR in Comparison With Quantitative Coronary Angiography. JACC: Cardiovascular Imaging, 2014, 7, 14-22.	5.3	97
139	Adiabatic inversion pulses for myocardial T1 mapping. Magnetic Resonance in Medicine, 2014, 71, 1428-1434.	3.0	119
140	Auto alibration approach for k–t SENSE. Magnetic Resonance in Medicine, 2014, 71, 1123-1129.	3.0	5
141	Phaseâ€sensitive inversion recovery for myocardial <i>T</i> ₁ mapping with motion correction and parametric fitting. Magnetic Resonance in Medicine, 2013, 69, 1408-1420.	3.0	90
142	T1 and extracellular volume mapping in the heart: estimation of error maps and the influence of noise on precision. Journal of Cardiovascular Magnetic Resonance, 2013, 15, 56.	3.3	143
143	Effectiveness of late gadolinium enhancement to improve outcomes prediction in patients referred for cardiovascular magnetic resonance after echocardiography. Journal of Cardiovascular Magnetic Resonance, 2013, 15, 6.	3.3	30
144	Influence of Off-resonance in myocardial T1-mapping using SSFP based MOLLI method. Journal of Cardiovascular Magnetic Resonance, 2013, 15, 63.	3.3	85

#	Article	IF	CITATIONS
145	High spatial and temporal resolution retrospective cine cardiovascular magnetic resonance from shortened free breathing real-time acquisitions. Journal of Cardiovascular Magnetic Resonance, 2013, 15, 102.	3.3	75
146	Design, evaluation and application of an eight channel transmit/receive coil array for cardiac MRI at 7.0T. European Journal of Radiology, 2013, 82, 752-759.	2.6	46
147	Real-time MRI-guided right heart catheterization in adults using passive catheters. European Heart Journal, 2013, 34, 380-389.	2.2	88
148	Myocardial T1 mapping and extracellular volume quantification: a Society for Cardiovascular Magnetic Resonance (SCMR) and CMR Working Group of the European Society of Cardiology consensus statement. Journal of Cardiovascular Magnetic Resonance, 2013, 15, 92.	3.3	864
149	Free-Breathing, Motion-Corrected Late Gadolinium Enhancement Is Robust and Extends Risk Stratification to Vulnerable Patients. Circulation: Cardiovascular Imaging, 2013, 6, 423-432.	2.6	59
150	Myocardial Damage Detected by Late Gadolinium Enhancement Cardiovascular Magnetic Resonance Is Associated With Subsequent Hospitalization for Heart Failure. Journal of the American Heart Association, 2013, 2, e000416.	3.7	39
151	MIA - A free and open source software for gray scale medical image analysis. Source Code for Biology and Medicine, 2013, 8, 20.	1.7	35
152	Integration of cardiac and respiratory motion into MRI roadmaps fused with xâ€ray. Medical Physics, 2013, 40, 032302.	3.0	33
153	Prevalence and Prognosis of Unrecognized Myocardial Infarction Determined by Cardiac Magnetic Resonance in Older Adults. JAMA - Journal of the American Medical Association, 2012, 308, 890.	7.4	234
154	Extracellular volume imaging by magnetic resonance imaging provides insights into overt and sub-clinical myocardial pathology. European Heart Journal, 2012, 33, 1268-1278.	2.2	482
155	Association Between Extracellular Matrix Expansion Quantified by Cardiovascular Magnetic Resonance and Short-Term Mortality. Circulation, 2012, 126, 1206-1216.	1.6	422
156	Comparison of three multichannel transmit/receive radiofrequency coil configurations for anatomic and functional cardiac MRI at 7.0T: implications for clinical imaging. European Radiology, 2012, 22, 2211-2220.	4.5	68
157	Automatic motion compensation of free breathing acquired myocardial perfusion data by using independent component analysis. Medical Image Analysis, 2012, 16, 1015-1028.	11.6	48
158	Cardiac imaging techniques for physicians: Late enhancement. Journal of Magnetic Resonance Imaging, 2012, 36, 529-542.	3.4	136
159	Extracellular volume fraction mapping in the myocardium, part 1: evaluation of an automated method. Journal of Cardiovascular Magnetic Resonance, 2012, 14, 60.	3.3	323
160	Extracellular volume fraction mapping in the myocardium, part 2: initial clinical experience. Journal of Cardiovascular Magnetic Resonance, 2012, 14, 61.	3.3	223
161	MultiContrast Delayed Enhancement (MCODE) improves detection of subendocardial myocardial infarction by late gadolinium enhancement cardiovascular magnetic resonance: a clinical validation study. Journal of Cardiovascular Magnetic Resonance, 2012, 14, 86.	3.3	420
162	A Quantitative Pixel-Wise Measurement of Myocardial Blood Flow by Contrast-Enhanced First-Pass CMR Perfusion Imaging. JACC: Cardiovascular Imaging, 2012, 5, 154-166.	5.3	120

PETER KELLMAN

#	Article	IF	CITATIONS
163	Myocardial Edema as Detected by Pre-Contrast T1 and T2 CMR Delineates Area at Risk Associated With Acute Myocardial Infarction. JACC: Cardiovascular Imaging, 2012, 5, 596-603.	5.3	283
164	Twoâ€Ðimensional sixteen channel transmit/receive coil array for cardiac MRI at 7.0 T: Design, evaluation, and application. Journal of Magnetic Resonance Imaging, 2012, 36, 847-857.	3.4	76
165	Motion correction for myocardial T1 mapping using image registration with synthetic image estimation. Magnetic Resonance in Medicine, 2012, 67, 1644-1655.	3.0	187
166	Retrospective reconstruction of high temporal resolution cine images from realâ€ŧime MRI using iterative motion correction. Magnetic Resonance in Medicine, 2012, 68, 741-750.	3.0	78
167	Motion correction for myocardial T1 mapping using image registration with synthetic image estimation. Magnetic Resonance in Medicine, 2012, 67, spcone.	3.0	2
168	Low b-Value Diffusion-Weighted Cardiac Magnetic Resonance Imaging. Investigative Radiology, 2011, 46, 751-758.	6.2	44
169	Myocardial extravascular extracellular volume fraction measurement by gadolinium cardiovascular magnetic resonance in humans: slow infusion versus bolus. Journal of Cardiovascular Magnetic Resonance, 2011, 13, 16.	3.3	198
170	Myocardial T1 and extracellular volume fraction mapping at 3 tesla. Journal of Cardiovascular Magnetic Resonance, 2011, 13, 75.	3.3	144
171	Edema by T2-weighted imaging in salvaged myocardium is extracellular, not intracellular. Journal of Cardiovascular Magnetic Resonance, 2011, 13, .	3.3	4
172	Temporal filtering effects in dynamic parallel MRI. Magnetic Resonance in Medicine, 2011, 66, 192-198.	3.0	13
173	Dynamic Changes of Edema and Late Gadolinium Enhancement After Acute Myocardial Infarction and Their Relationship to Functional Recovery and Salvage Index. Circulation: Cardiovascular Imaging, 2011, 4, 228-236.	2.6	214
174	Bright-Blood T ₂ -Weighted MRI Has High Diagnostic Accuracy for Myocardial Hemorrhage in Myocardial Infarction. Circulation: Cardiovascular Imaging, 2011, 4, 738-745.	2.6	57
175	Nonrigid Motion Compensation of Free Breathing Acquired Myocardial Perfusion Data. Informatik Aktuell, 2011, , 84-88.	0.6	5
176	Myocardial Fat Imaging. Current Cardiovascular Imaging Reports, 2010, 3, 83-91.	0.6	72
177	Exploiting Quasiperiodicity in Motion Correction of Free-Breathing Myocardial Perfusion MRI. IEEE Transactions on Medical Imaging, 2010, 29, 1516-1527.	8.9	26
178	Chemical shift–based water/fat separation: A comparison of signal models. Magnetic Resonance in Medicine, 2010, 64, 811-822.	3.0	116
179	Simultaneous myocardial strain and darkâ€blood perfusion imaging using a displacementâ€encoded MRI pulse sequence. Magnetic Resonance in Medicine, 2010, 64, 787-798.	3.0	7

180 On Breathing Motion Compensation in Myocardial Perfusion Imaging. , 2010, , .

2

#	Article	IF	CITATIONS
181	Magnetic Resonance Imaging Delineates the Ischemic Area at Risk and Myocardial Salvage in Patients With Acute Myocardial Infarction. Circulation: Cardiovascular Imaging, 2010, 3, 527-535.	2.6	114
182	Coronary MRA at 3 T using 3d multi-interleaved multi-echo acquisition with varpro fat-water separation. Journal of Cardiovascular Magnetic Resonance, 2010, 12, .	3.3	2
183	Late Gadolinium-Enhancement Cardiac Magnetic Resonance Identifies Postinfarction Myocardial Fibrosis and the Border Zone at the Near Cellular Level in Ex Vivo Rat Heart. Circulation: Cardiovascular Imaging, 2010, 3, 743-752.	2.6	156
184	Virtual coil concept for improved parallel MRI employing conjugate symmetric signals. Magnetic Resonance in Medicine, 2009, 61, 93-102.	3.0	83
185	Multiecho dixon fat and water separation method for detecting fibrofatty infiltration in the myocardium. Magnetic Resonance in Medicine, 2009, 61, 215-221.	3.0	115
186	HTGRAPPA: Realâ€time <i>B</i> ₁ â€weighted image domain TGRAPPA reconstruction. Magnetic Resonance in Medicine, 2009, 61, 1425-1433.	3.0	10
187	High spatial and temporal resolution cardiac cine MRI from retrospective reconstruction of data acquired in real time using motion correction and resorting. Magnetic Resonance in Medicine, 2009, 62, 1557-1564.	3.0	87
188	Variability of myocardial perfusion dark rim Gibbs artifacts due to sub-pixel shifts. Journal of Cardiovascular Magnetic Resonance, 2009, 11, 17.	3.3	34
189	Variability of perfusion dark rim artifacts due to Gibbs ringing. Journal of Cardiovascular Magnetic Resonance, 2009, 11, .	3.3	ο
190	Improved image reconstruction incorporating non-rigid motion correction for cardiac MRI using BLADE acquisition. Journal of Cardiovascular Magnetic Resonance, 2009, 11, .	3.3	4
191	Unsupervised Inline Analysis of Cardiac Perfusion MRI. Lecture Notes in Computer Science, 2009, 12, 741-749.	1.3	31
192	Nonlinear myocardial signal intensity correction improves quantification of contrastâ€enhanced firstâ€pass MR perfusion in humans. Journal of Magnetic Resonance Imaging, 2008, 27, 793-801.	3.4	56
193	ACUT ₂ E TSEâ€SFP: A hybrid method for T2â€weighted imaging of edema in the heart. Magnetic Resonance in Medicine, 2008, 59, 229-235.	3.0	536
194	Fully automatic, retrospective enhancement of realâ€time acquired cardiac cine MR images using imageâ€based navigators and respiratory motionâ€corrected averaging. Magnetic Resonance in Medicine, 2008, 59, 771-778.	3.0	64
195	Semiautomated Segmentation of Myocardial Contours for Fast Strain Analysis in Cine Displacement-Encoded MRI. IEEE Transactions on Medical Imaging, 2008, 27, 1084-1094.	8.9	65
196	Parallelized Hybrid TGRAPPA Reconstruction for Real-Time Interactive MRI. Lecture Notes in Computer Science, 2008, 11, 163-170.	1.3	0
197	Imaging Sequences for First Pass Perfusion - A Review. Journal of Cardiovascular Magnetic Resonance, 2007, 9, 525-537.	3.3	126
198	Improved cine displacement-encoded MRI using balanced steady-state free precession and time-adaptive sensitivity encoding parallel imaging at 3 T. NMR in Biomedicine, 2007, 20, 591-601.	2.8	419

#	Article	IF	CITATIONS
199	T2-prepared SSFP improves diagnostic confidence in edema imaging in acute myocardial infarction compared to turbo spin echo. Magnetic Resonance in Medicine, 2007, 57, 891-897.	3.0	219
200	Motion corrected freeâ€breathing delayedâ€enhancement imaging of myocardial infarction using nonrigid registration. Journal of Magnetic Resonance Imaging, 2007, 26, 184-190.	3.4	470
201	Direct comparison of myocardial perfusion cardiovascular magnetic resonance sequences with parallel acquisition. Journal of Magnetic Resonance Imaging, 2007, 26, 1444-1451.	3.4	25
202	Phased array ghost elimination. NMR in Biomedicine, 2006, 19, 352-361.	2.8	31
203	T2* measurement during first-pass contrast-enhanced cardiac perfusion imaging. Magnetic Resonance in Medicine, 2006, 56, 1132-1134.	3.0	24
204	Quantitative myocardial infarction on delayed enhancement MRI. Part II: Clinical application of an automated feature analysis and combined thresholding infarct sizing algorithm. Journal of Magnetic Resonance Imaging, 2006, 23, 309-314.	3.4	77
205	Quantitative myocardial infarction on delayed enhancement MRI. Part I: Animal validation of an automated feature analysis and combined thresholding infarct sizing algorithm. Journal of Magnetic Resonance Imaging, 2006, 23, 298-308.	3.4	154
206	Quantitative myocardial perfusion analysis with a dual-bolus contrast-enhanced first-pass MRI technique in humans. Journal of Magnetic Resonance Imaging, 2006, 23, 315-322.	3.4	130
207	Multicontrast delayed enhancement provides improved contrast between myocardial infarction and blood pool. Journal of Magnetic Resonance Imaging, 2005, 22, 605-613.	3.4	46
208	Preliminary investigation of respiratory self-gating for free-breathing segmented cine MRI. Magnetic Resonance in Medicine, 2005, 53, 159-168.	3.0	172
209	Motion-corrected free-breathing delayed enhancement imaging of myocardial infarction. Magnetic Resonance in Medicine, 2005, 53, 194-200.	3.0	115
210	Dynamic autocalibrated parallel imaging using temporal GRAPPA (TGRAPPA). Magnetic Resonance in Medicine, 2005, 53, 981-985.	3.0	611
211	Real-time blood flow imaging using autocalibrated spiral sensitivity encoding. Magnetic Resonance in Medicine, 2005, 54, 1557-1561.	3.0	29
212	Image reconstruction in SNR units: A general method for SNR measurement. Magnetic Resonance in Medicine, 2005, 54, 1439-1447.	3.0	443
213	Single heartbeat cardiac tagging for the evaluation of transient phenomena. Magnetic Resonance in Medicine, 2005, 54, 1455-1464.	3.0	10
214	Temporal dynamics of the BOLD fMRI impulse response. NeuroImage, 2005, 24, 667-677.	4.2	110
215	Real-time, Interactive MRI for Cardiovascular Interventions1. Academic Radiology, 2005, 12, 1121-1127.	2.5	36
216	Artifact suppression in imaging of myocardial infarction usingB1-weighted phased-array combined phase-sensitive inversion recovery. Magnetic Resonance in Medicine, 2004, 51, 408-412.	3.0	20

#	Article	IF	CITATIONS
217	Real time high spatial-temporal resolution flow imaging with spiral MRI using auto-calibrated SENSE. , 2004, 2004, 1914-7.		3
218	Gadolinium delayed enhancement cardiovascular magnetic resonance correlates with clinical measures of myocardial infarction. Journal of the American College of Cardiology, 2004, 43, 2253-2259.	2.8	292
219	Hunting for neuronal currents: absence of rapid MRI signal changes during visual-evoked response. NeuroImage, 2004, 23, 1059-1067.	4.2	71
220	Automatic in-plane rotation for doubly-oblique cardiac imaging. Journal of Magnetic Resonance Imaging, 2003, 18, 612-615.	3.4	1
221	Real-time accelerated interactive MRI with adaptive TSENSE and UNFOLD. Magnetic Resonance in Medicine, 2003, 50, 315-321.	3.0	87
222	Assessment of regional systolic and diastolic dysfunction in familial hypertrophic cardiomyopathy using MR tagging. Magnetic Resonance in Medicine, 2003, 50, 638-642.	3.0	102
223	Method for functional MRI mapping of nonlinear response. NeuroImage, 2003, 19, 190-199.	4.2	26
224	Phase-sensitive inversion recovery for detecting myocardial infarction using gadolinium-delayed hyperenhancement. Magnetic Resonance in Medicine, 2002, 47, 372-383.	3.0	941
225	Multishot EPI-SSFP in the heart. Magnetic Resonance in Medicine, 2002, 47, 655-664.	3.0	40
226	Application of sensitivity-encoded echo-planar imaging for blood oxygen level-dependent functional brain imaging. Magnetic Resonance in Medicine, 2002, 48, 1011-1020.	3.0	142
227	Phased array ghost elimination (PACE) for segmented SSFP imaging with interrupted steady-state. Magnetic Resonance in Medicine, 2002, 48, 1076-1080.	3.0	9
228	Adaptive sensitivity encoding incorporating temporal filtering (TSENSE). Magnetic Resonance in Medicine, 2001, 45, 846-852.	3.0	764
229	Chost artifact cancellation using phased array processing. Magnetic Resonance in Medicine, 2001, 46, 335-343.	3.0	40
230	Low latency temporal filter design for real-time MRI using UNFOLD. Magnetic Resonance in Medicine, 2000, 44, 933-939.	3.0	16